

Wrinkling Analysis in a Film Bonded to a Compressible Compliant Substrate in Large Deformation

Zhicheng Ou¹, Xiaohu Yao¹, Xiaoqing Zhang^{1,2} and Xuejun Fan³

Abstract: The buckling of a thin film on a compressible compliant substrate in large deformation is studied. A finite-deformation theory is developed to model the film and the substrate under different original strain-free configurations. The neo-Hookean constitutive relation is applied to describe the substrate. Through the perturbation analysis, the analytical solution for this highly nonlinear system is obtained. The buckling wave number, amplitude and critical condition are obtained. Comparing with the traditional linear model, the buckling amplitude decreases. The wave number increases and relates to the prestrain. With the increment of Poisson's ratio of the substrate, the buckling wave number increases, but the amplitude decreases. The displacements near the interface are different in two models.

Keywords: film, substrate, buckling, large deformation, neo-Hookean.

1 Introduction

Stretchable electronics is now attracting considerable attention, due to its broad range of applications, such as microelectronics, medicine, clothing and military. Comparing with traditional printing and flat panel displays, flexible displays have both of their advantages, which are soft and portable, and able to store more information [Rogers and Bao (2002)]. The flexible sensors integrated into the clothes can monitor the health information of human body [Wagner, Lacour, Jones, Hsu, Sturm, Li and Suo (2004)]. Travelers and athletes can carry flexible solar panels for power [Schubert and Werner (2006)]. To make the device stretchable, buckling of a stiff film bound to a compliant substrate is applied. Khang, Jiang, Huang and Rogers (2006) produced a stretchable form of silicon based on a PDMS substrate. It is periodic and wavelike in microscale. It can be reversibly stretched and compressed in large deformation without damage.

¹ School of Civil Engineering and Transportation, South China University of Technology, Guangzhou 510640, PR China.

² Corresponding author. E-mail: tcqzhang@scut.edu.cn

³ Department of Mechanical Engineering, Lamar University, Beaumont, TX, 77710, USA.

Huang, Hong and Suo (2005) developed a model of a stiff elastic thin film on a compliant elastic substrate subjected to an axial strain. They obtained the buckling wavelength and amplitude of the film and developed a method to reveal the two-dimensional patterns. Huang (2005) studied the wrinkling process of an elastic film on a viscoelastic layer. Linear perturbation analysis is conducted to reveal the kinetics of wrinkling in the film. Huang and Suo (2002) studied the wrinkling process of this system by using the lubrication theory for the viscous flow and the nonlinear plate theory for the elastic film, and presented a more rigorous analysis for all thickness range of the viscous layer. Im and Huang (2008) considered the wrinkle patterns of anisotropic crystal films on viscoelastic substrates. Jiang, Khang, Fei, Kim, Huang, Xiao and Rogers (2008) considered the finite width effect of thin-films buckling on compliant substrate. Song, Jiang, Choi, Khang, Huang and Rogers (2008) studied the two-dimensional buckling including checkerboard and herringbone modes, and found that the herringbone mode corresponds to the lowest energy, as observed in experiments. Chen and Hutchinson (2004) also showed that the herringbone mode constituted a minimum energy configuration among a limited set of competing modes. Audoly and Boudaoud (2008) studied the secondary instabilities of these modes and presented a weakly nonlinear post-buckling analysis. They found that the square checkerboard mode was optimal just above the threshold under equi-biaxial prestrain. Cai, Breid, Crosby, Suo and Hutchinson (2011) studied the thin stiff films on compliant elastic substrates subjected to equi-biaxial compressive stress states, which were observed to buckle into various periodic patterns including checkerboard, hexagonal and herringbone. For flat films, the checkerboard mode was preferred only above the threshold. Nair, Farkas and Kriz (2008) studied of size effects and deformation of thin films due to nanoindentation using molecular dynamics simulations. Kurapati, Lu and Yang (2010) used the finite element method to analyze the spherical indentation of elastic film and substrate structures.

In previous studies, the substrate is usually described by small deformation theory and linear elastic constitutive relation. But when the structure are subjected to large loads and buckles into large deformation, the small deformation hypothesis is no longer applicable. Song, Jiang, Liu, Khang, Huang, Rogers, Lu and Koh (2008) analyzed the large deformation of this structure by perturbation method. The original strain-free configuration of the film was considered. The finite strain theory and hyperelasticity constitutive relation were applied to describe the substrate. For the incompressible substrate, the buckling features were deduced analytically and coincided well with the experiments and simulations. Zhu, Zhou and Fan (2014) studied rupture and instability of soft films due to moisture vaporization in micro-electronic devices. Neo-Hookean, Mooney–Rivlin, and Ogden’s models were used

to derive the analytical solutions. Zhang and Yang (2013) studied the methods of extracting the mechanical properties of nonlinear elastic materials under large deformation and built general relationships of the indentation load and depth of hyperelastic materials.

This paper focuses on the case of compressible substrate. The displacements in the linear and nonlinear models are compared. The influence of the compressibility of the substrate on buckling is discussed. The coordinate systems are based on the original strain-free configurations of the film and the substrate. A hyperelasticity, neo-Hookean, constitutive relation is applied to describe the substrate under finite deformation theory. Through the perturbation analysis, the displacement of substrate is solved analytically. The buckling wave number, amplitude and critical condition are obtained by energy method. Comparing with the traditional linear model, the buckling amplitude in the nonlinear model decreases. The wave number increases and relates to the prestrain. With the increment of Poisson's ratio of the substrate, the buckling wave number increases, but the amplitude decreases. The displacements near the interface in two models are different.

2 Displacement

2.1 Model

A stiff elastic thin film is bonded to a compliant elastic thick substrate without slipping, as shown in Fig. 1. H and h are the thickness of the substrate and the film, respectively, and $H \gg h$. The substrate is imposed a uniaxial prestrain ε_0 first, and then is bonded to a stress-free film, as shown in Fig. 1(a). After the prestrain in the substrate released, the structure buckles, as shown in Fig. 1(b). Since the structure is only imposed a uniaxial load and the length (x_2) is much larger than the buckling amplitude, the substrate can be simplified as a plane strain problem, and the thin film can be modeled as a beam undergoing large rotation. The Young's modulus and Poisson's ratio of the film and substrate are E_f and ν_f and E and ν . The film is much harder than the substrate, so $E_f \gg E$.

The original strain-free states of the film and the substrate are asynchronous, as shown in Fig. 2. In the first step, Fig. 2(a), the substrate is strain-free with the original length l . In the second step, Fig. 2(b), the substrate is stretched to the length $(1+\varepsilon_0)l$ with a prestrain ε_0 , but the film is free with the original length l and attached to the substrate. In the third step, Fig. 2(c), the substrate is relaxed to its original length l , and the film buckles under compression. Two coordinate systems are based on the strain-free configurations of the film and the substrate, as shown in Fig. 2(a) and (b), with the transformation: $x_1 = \xi x'_1 = x'_1(1 + \varepsilon_0)^{-1}$.

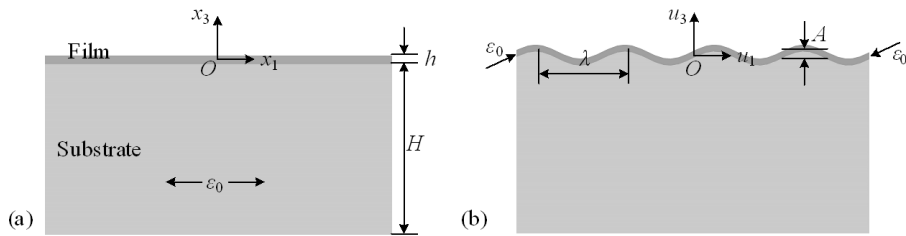


Figure 1: A stiff thin film on a compliant thick substrate: (a) The film is bonded to a pre-strained substrate; (b) The structure buckles after releasing the prestrain.

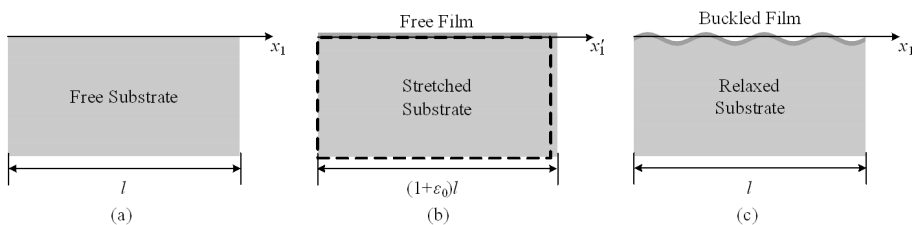


Figure 2: The buckling process and coordinate systems (a) Free substrate; (b) Stretched substrate and free film; (c) Relaxed substrate and buckled film.

In this paper, two models are compared:

(1) Linear model. The small deformation theory and linear elasticity constitutive relation, Hookean law, are applied to describe the substrate. The same coordinate system under the strain-free configuration of the substrate is applied to describe the film and the substrate.

(2) Nonlinear model. The finite deformation theory and nonlinear hyperelasticity constitutive relation, neo-Hookean law, are applied to describe the substrate. Different coordinate systems under the strain-free configurations of the film and the substrate are applied.

2.2 Film

Under the coordinate system based on the strain-free configuration of the film, Fig. 2(b) the in-plane displacement and deflection in the midplane are denoted by u_1 and u_3 respectively and they are independent of the thickness. When the film buckles, it undergoes large rotation, so the influence of the deflection should be considered

According to the finite deformation theory, the axial strain is

$$\varepsilon_{11} = \frac{du_1}{dx'_1} + \frac{1}{2} \left(\frac{du_3}{dx'_1} \right)^2 \quad (1)$$

The membrane force is given by Hookean law (plane stress) as

$$N_{11} = h\sigma_{11} = h\bar{E}_f \varepsilon_x. \quad (2)$$

where effective modulus is $\bar{E}_f = E_f/(1 - \nu_f^2)$. The shear traction at the interface is too small to be neglected [Huang, Hong and Suo (2005)], so the equilibrium equation is

$$T_1 = \frac{dN_{11}}{dx'_1} = 0 \quad (3)$$

The uniaxial buckling mode is assumed as a cosine curve, the deflection of the film is assumed as

$$u_3 = A \cos(kx_1) = A \cos(\xi k x'_1) \quad (4)$$

where A and k are the amplitude and wave number in the buckled configuration, Fig. 2(c). The wavelength is assumed much larger than the film thickness and amplitude, $\lambda = 2\pi/k \gg A, h$, or $Ak, hk \ll 1$. From Eqs.(1)~(4), the in-plane displacement is obtained,

$$u_1 = \frac{1}{8} \xi A^2 k \sin(2k\xi x'_1) - \varepsilon_0 \xi x'_1 = \frac{1}{8} \xi A^2 k \sin(2kx_1) - \varepsilon_0 x_1 \quad (5)$$

The midplane displacement consists of two parts. One is the axial displacement $-\varepsilon x$ caused by axial compression the other is the wavy displacement caused by buckling.

The strain energy is the sum of bending and stretching contribution. Their strain energy densities are

$$W_b = \frac{h^3 \bar{E}_f}{24} \left(\frac{d^2 u_3}{dx'^2_1} \right)^2, \quad W_m = \frac{1}{2} \sigma_{11} \varepsilon_{11} \quad (6)$$

After integration, the strain energy of the film is

$$U_f = \int_0^{l/\xi} (W_b + W_m) dx'_1 = \frac{1}{96} \xi \bar{E}_f h l [3(\xi A^2 k^2 - 4\varepsilon_0)^2 + 2\xi^2 A^2 k^4 h^2] \quad (7)$$

In traditional analysis, the strain-free configuration of the film is the same as the substrate, so $\xi = 1$.

2.3 Substrate

Under the coordinate system based on the strain-free configuration of the substrate, Fig. 2(a), the displacement is denoted by u_I ($I=1,3$). The deformation gradient is $F_{IJ} = \delta_{IJ} + u_{IJ}$. The Green strain tensor is

$$E_{IJ} = \frac{1}{2}(u_{I,J} + u_{J,I} + u_{K,I}u_{K,J}) \quad (8)$$

Nonlinear constitutive relation is used,

$$T_{IJ} = \frac{\partial W_s}{\partial E_{IJ}} \quad (9)$$

where W_s is the strain energy density, and T_{IJ} is the 2nd Piola–Kirchhoff stress. In neo-Hookean constitutive law, the strain energy density has the form that

$$W_s = C_1(J^{-2/3}I_1 - 3) + D_1(J - 1)^2 \quad (10)$$

where the material constants are $C_1 = E/4(1+\nu)$, $D_1 = E/6(1-2\nu)$. J is the volume change at a point and equals to the determinant of deformation gradient \mathbf{F} , $J = \det \mathbf{F} = |\delta_{IJ} + 2E_{IJ}|^{1/2}$. The first invariant I_1 is the trace of the left Cauchy–Green strain tensor, that is $I_1 = \text{tr} \mathbf{B} = \text{tr} \mathbf{F} \mathbf{F}^T = \delta_{II} + 2\text{tr} \mathbf{E}$. Specially, for the incompressible material, $J = 1$, the strain energy density can be simplified as $W_s = C_1(I_1 - 3)$. The force equilibrium equation and the traction on the surface are

$$(F_{IK}T_{JK})_{,J} = 0, \quad T_I = F_{IK}T_{JK}n_J \quad (11)$$

where n_J is the unit normal vector of the surface. In plane strain problem, the equations above can be simplified. The volume change J and the first invariant I_1 are

$$J^2 = 1 + 2E_{11} + 2E_{33} + 4E_{11}E_{33} - 4E_{13}E_{31}, \quad I_1 = 3 + 2E_{11} + 2E_{33} \quad (12)$$

By substituting Eq.(12) into Eqs. (9)~(10), the 2nd Piola–Kirchhoff stress components are obtained,

$$\begin{cases} T_{11} = \frac{2}{3J^{4/3}} [C_1(1 + 4E_{11} + 8E_{11}E_{33} - 4E_{33}^2 - 12E_{13}^2) + 3D_1J^{1/3}(J - 1)(1 + 2E_{33})] \\ T_{33} = \frac{2}{3J^{4/3}} [C_1(1 + 4E_{33} + 8E_{11}E_{33} - 4E_{11}^2 - 12E_{13}^2) + 3D_1J^{1/3}(J - 1)(1 + 2E_{11})] \\ T_{13} = T_{31} = \frac{4}{3J^{4/3}} [2C_1E_{13}(1 + E_{11} + E_{33}) - 3D_1J^{1/3}(J - 1)E_{13}] \end{cases} \quad (13)$$

From Eq.(11), the equilibrium equations and tractions are expanded,

$$\begin{cases} (F_{11}T_{11} + F_{13}T_{13})_{,1} + (F_{11}T_{31} + F_{13}T_{33})_{,3} = 0 \\ (F_{31}T_{11} + F_{33}T_{13})_{,1} + (F_{31}T_{31} + F_{33}T_{33})_{,3} = 0 \end{cases} \quad (14)$$

$$T_1 = F_{11}T_{31} + F_{13}T_{33}, \quad T_3 = F_{31}T_{31} + F_{33}T_{33} \quad (15)$$

The bottom of the substrate is free. At the interface, the shear traction is neglected, and the normal displacement is continuous. The boundary conditions are

$$x_3 = -H : T_1 = T_3 = 0; \quad x_3 = 0 : u_3 = A \cos(kx_1), \quad T_1 = 0 \quad (16)$$

From Eq.(8), equilibrium equations (14) can be simplified as a boundary value problem about the displacement. The perturbation method is applied to solve this highly nonlinear problem. Since the amplitude A is much smaller than the wavelength λ , a small dimensionless parameter $\delta = A/\lambda$ is used to expand the displacement to power series,

$$\begin{cases} u_1(x_1, x_3) = A \left[u_{10}(x_1, x_3) + \delta u_{11}(x_1, x_3) + \delta^2 u_{12}(x_1, x_3) + \dots \right] \\ u_3(x_1, x_3) = A \left[u_{30}(x_1, x_3) + \delta u_{31}(x_1, x_3) + \delta^2 u_{32}(x_1, x_3) + \dots \right] \end{cases} \quad (17)$$

By substituting Eq.(17) into (14)~(16), the displacement in each order can be solved

$$u_{10} = \frac{1-2\nu+kx_3}{2-2\nu} e^{kx_3} \sin(kx_1); \quad u_{30} = \left(1 + \frac{kx_3}{2-2\nu} \right) e^{kx_3} \cos(kx_1) \quad (18)$$

$$\begin{aligned} u_{11} &= \frac{\pi}{144(1-\nu)^3} e^{2kx_3} \sin(2kx_1) [2kx_3(80\nu^3 - 96\nu^2 + 81\nu - 40) - 80\nu^3 + 24\nu^2 + 63\nu - 32] \\ u_{31} &= -\frac{\pi}{144(1-\nu)^3} \left\{ 2kx_3 e^{2kx_3} [(80\nu^3 - 96\nu^2 + 81\nu - 40) \cos(2kx_1) + 3kx_3(8\nu - 7) \right. \\ &\quad \left. + 6(8\nu^2 - 15\nu + 7)] + (1 - e^{2kx_3})(160\nu^3 - 144\nu^2 + 30\nu + 1) \right\} \end{aligned} \quad (19)$$

$$\begin{aligned} u_{12} &= \frac{\pi^2}{248832(1-\nu)^5} e^{kx_3} \left\{ 64e^{2kx_3} \sin(3kx_1) [3kx_3(640\nu^5 + 6544\nu^4 - 13704\nu^3 + 10642\nu^2 \right. \\ &\quad - 4403\nu + 906) - 3520\nu^5 + 1808\nu^4 + 4344\nu^3 - 4774\nu^2 + 1739\nu - 222] \\ &\quad + 9e^{2kx_3} \sin(kx_1) [72k^3 x_3^3 (8\nu - 7) + 4k^2 x_3^2 (5120\nu^4 - 13056\nu^3 + 18720\nu^2 - 15196\nu \\ &\quad + 4797) + kx_3(40960\nu^5 - 114688\nu^4 + 134656\nu^3 - 102368\nu^2 + 55208\nu - 14171) \\ &\quad - 10240\nu^5 + 108544\nu^4 - 106816\nu^3 - 27520\nu^2 + 65506\nu - 20065] \\ &\quad \left. - 9\sin(kx_1) [kx_3(25600\nu^4 - 39680\nu^3 + 6816\nu^2 + 12592\nu - 4991) + 71680\nu^5 \right. \\ &\quad \left. + 62464\nu^4 - 186048\nu^3 + 67840\nu^2 + 24094\nu - 12543] \right\} \end{aligned} \quad (20)$$

$$\begin{aligned}
u_{32} = & -\frac{\pi^2}{82944(1-\nu)^5} e^{kx_3} \left\{ 64kx_3 e^{2kx_3} \cos(3kx_1) (640v^5 + 6544v^4 - 13704v^3 + 10642v^2 \right. \\
& - 4403v + 906) + 3e^{2kx_3} \cos(kx_1) [24k^3 x_3^3 (256v^2 - 456v + 209) \\
& + 36k^2 x_3^2 (5120v^4 - 8960v^3 + 7456v^2 - 4820v + 1607) \\
& + kx_3 (40960v^5 - 65536v^4 + 77824v^3 - 121760v^2 + 97544v - 27161) \\
& + 2(87040v^5 - 86528v^4 + 1215 - 19872v^3 + 48880v^2 - 16823v)] \\
& - 3 \cos(kx_1) [kx_3 (25600v^4 - 39680v^3 + 6816v^2 + 12592v - 4991) \\
& \left. + 2(87040v^5 - 86528v^4 - 19872v^3 + 48880v^2 - 16823v + 1215)] \right\} \quad (21)
\end{aligned}$$

In the linear model, the displacement is the first order of displacement, that is Eq.(18). In the nonlinear model, the tangential displacement u_1 at the surface ($z=0$) is

$$\begin{aligned}
u_1^* = & -\frac{1}{497664(1-\nu)^5} A^3 k^2 [9 \sin(kx_1) (40960v^5 - 23040v^4 - 39616v^3 + 47680v^2 \\
& - 20706v + 3761) + 32 \sin(3kx_1) (3520v^5 - 1808v^4 - 4344v^3 + 4774v^2 - 1739v \\
& + 222)] - \frac{80v^3 - 24v^2 - 63v + 32}{288(1-\nu)^3} A^2 k \sin(2kx_1) + \frac{1-2\nu}{2(1-\nu)} A \sin(kx_1) \quad (22)
\end{aligned}$$

In the linear model, u_1^* is the first term in Eq.(22)

By substituting the displacements (18)~(21) into Eqs. (8) and (10), the strain energy can be integrated as

$$U_s = \int_{-H}^0 \int_0^l W_s dx_1 dx_3 = \frac{1}{8} \bar{E}_s l k A^2 (1 + \gamma A^2 k^2) \quad (23)$$

$$\gamma = \frac{2607 - 14720v + 29984v^2 - 7296v^3 - 52736v^4 + 51200v^5}{55296(1-\nu)^4} \quad (24)$$

where the effective modulus is $\bar{E}_s = E/(1-\nu^2)$. In the linear model, the strain energy is the first term of Eq.(23), or $\gamma = 0$. For the incompressible substrate ($\nu=1/2$ and $\gamma = 5/128$), the displacements in the nonlinear model are

$$\begin{aligned}
u_1 = & Akx_3 e^{kx_3} \sin(kx_1) - \frac{1}{8} A^2 k e^{2kx_3} (6kx_3 + 1) \sin(2kx_1) \\
& + \frac{1}{32} A^3 k^2 e^{kx_3} \left\{ 64kx_3 e^{2kx_3} \sin(3kx_1) \right. \\
& \left. + \sin(kx_1) [13kx_3 + 24 - e^{2kx_3} (8k^3 x_3^3 - 84k^2 x_3^2 + 45kx_3 + 40)] \right\}
\end{aligned}$$

$$\begin{aligned}
u_3 = & A e^{kx_3} (1 - kx_3) \cos(kx_1) + \frac{1}{4} A^2 k^2 e^{2kx_3} x_3 [2kx_3 - 2 + 3 \cos(2kx_1)] \\
& - \frac{1}{32} A^3 k^2 e^{kx_3} \left\{ 64kx_3 e^{2kx_3} \cos(3kx_1) + \cos(kx_1) [13kx_3 + 11 \right. \\
& \left. + e^{2kx_3} (40k^3 x_3^3 + 116k^2 x_3^2 - 71kx_3 - 11)] \right\}
\end{aligned} \quad (25)$$

And the strain energy is

$$U_s = \frac{1}{6} E k l A^2 \left(1 + \frac{5}{128} A^2 k^2 \right) \quad (26)$$

Song, Jiang, Liu, Khang, Huang, Rogers, Lu and Koh (2008) have the same result when the substrate is incompressible.

3 Buckling

From Eqs. (7) and (23), the total potential energy of the film and substrate is

$$\begin{aligned}
U &= U_f + U_s \\
&= \frac{1}{32} l k^3 A^4 (4\gamma \bar{E}_s + \xi^3 k h \bar{E}_f) + \frac{1}{48} l k A^2 [6\bar{E}_s + \bar{E}_f h k \xi^2 (\xi k^2 h^2 - 12\varepsilon_0)] + \frac{1}{2} \xi l h \bar{E}_f \varepsilon_0^2
\end{aligned} \quad (27)$$

According to the principle of minimum potential energy, the buckling government equations are deduced by minimizing the total energy (27), that is $\partial U / \partial A = \partial U / \partial k = 0$,

$$\begin{cases} \mu (1 + \gamma A^2 k^2) - (\xi k h)^3 = 0 \\ \mu (3 + 5\gamma A^2 k^2) + 3\xi^2 h k (\xi A^2 k^2 - 4\varepsilon_0) = 0 \end{cases} \quad (28)$$

where the relative effective modulus is $\mu = 3\bar{E}_s / \bar{E}_f \ll 1$. If setting $\xi = 1$ and $\gamma = 0$, Eqs. (28) degenerates to the case of the linear model: $\mu - h^3 k^3 = 0$; $\mu + h k (A^2 k^2 - 4\varepsilon_0) = 0$. It is easy to solve the buckling wave number, critical prestrain and amplitude,

$$\bar{k} = \frac{1}{h} \mu^{1/3}, \quad \bar{\varepsilon}_0 = \frac{1}{4} \mu^{2/3}, \quad \bar{A} = h \sqrt{\frac{\varepsilon_0}{\bar{\varepsilon}_0} - 1} \quad (29)$$

The variable with a bar indicates the result in the linear model. The wave number only relates to the material property but not to prestrain. By substituting Eq. (29) into (27), the minimum potential energy in the linear model is

$$\bar{U} = \frac{1}{32} h l \bar{E}_f \mu^{2/3} (8\varepsilon_0 - \mu^{2/3}) \quad (30)$$

In the nonlinear model, the critical prestrain is deduced by setting $A=0$ in Eq. (28),

$$\tilde{\epsilon}_0 = \frac{\mu^{2/3}}{4 - \mu^{2/3}} = \frac{\bar{\epsilon}_0}{1 - \bar{\epsilon}_0} \approx \bar{\epsilon}_0 \tag{31}$$

It is only dependent on the material property and approximate to the critical prestrain in the linear model. The ratios between the linear and nonlinear model of the buckling amplitude and wave number are assumed that $\tilde{A}=\alpha\bar{A}$, $\tilde{k}=\kappa\bar{k}$. The variable with a tilde indicates the result in the nonlinear model. From Eq. (29), the buckling government equations (28) can expressed about the parameters α and κ ,

$$\begin{cases} 1 - \xi^3 \kappa^3 + \alpha^2 \kappa^2 \gamma (4\epsilon_0 - \mu^{2/3}) = 0 \\ 3\mu^{2/3} - 12\xi^2 \kappa \epsilon_0 + \alpha^2 \kappa^2 (5\gamma\mu^{2/3} + 3\xi^3 \kappa) (4\epsilon_0 - \mu^{2/3}) = 0 \end{cases} \tag{32}$$

Neglecting the small quantity μ (when the prestrain is not too small), the parameters are solved,

$$\kappa \approx (1 + \epsilon_0) [4\gamma\epsilon_0(1 + \epsilon_0) + 1]^{1/3}, \quad \alpha \approx (1 + \epsilon_0)^{-1/2} [4\gamma\epsilon_0(1 + \epsilon_0) + 1]^{-1/3} \tag{33}$$

By substituting Eqs. (29), (30) and (33) into (27), the minimum potential energy in the nonlinear model $\tilde{U} = \phi\bar{U}$ is obtained. The ratio between two models is

$$\phi \approx [4\gamma\epsilon_0(1 + \epsilon_0) + 1]^{2/3} \tag{34}$$

From Eqs. (29), (30), (33) and (34), the buckling wave number, amplitude and critical prestrain and minimum potential energy are

$$\tilde{k} = \frac{(1 + \epsilon_0)\zeta}{h}, \quad \tilde{A} = \frac{h}{\zeta} \sqrt{\frac{4\epsilon_0 - \mu^{2/3}}{1 + \epsilon_0}}, \quad \tilde{\epsilon}_0 = \frac{\mu^{2/3}}{4 - \mu^{2/3}}, \quad \tilde{U} = \frac{\zeta^2 h l \bar{E}_f}{32} (8\epsilon_0 - \mu^{2/3}) \tag{35}$$

where $\zeta = [4\mu\gamma\epsilon_0(1+\epsilon_0) + \mu]^{1/3}$. Different from the linear model, the buckling wave number is not only dependent on the material properties but also the prestrain.

4 Discussion

4.1 Substrate

The displacement fields of the substrate in linear and nonlinear models are compared by setting $A= 3 \mu\text{m}$, $k= 0.367 \mu\text{m}^{-1}$ ($\delta = 0.175$) and $\nu= 1/2$, as shown in Fig. 3 and 4 At the top of the substrate (the interface to the film), the distribution of displacement in two models is different. The spatial period (x_1) in the nonlinear model is nearly two times as that in the linear model. From Eq. (22), the tangential

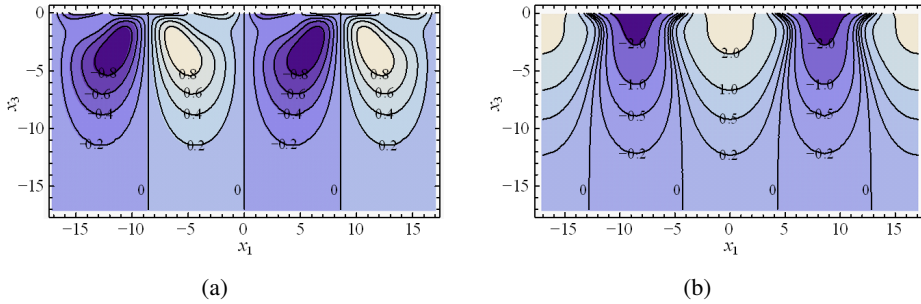


Figure 3: Displacements (a) u_1 and (b) u_3 of the substrate in the nonlinear model (μm).

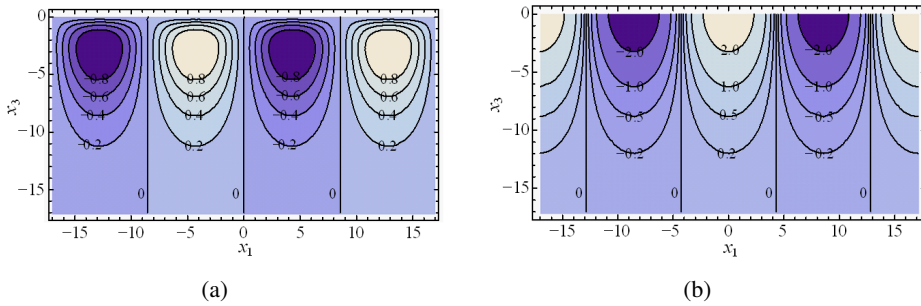


Figure 4: Displacements (a) u_1 and (b) u_3 of the substrate in the linear model (μm).

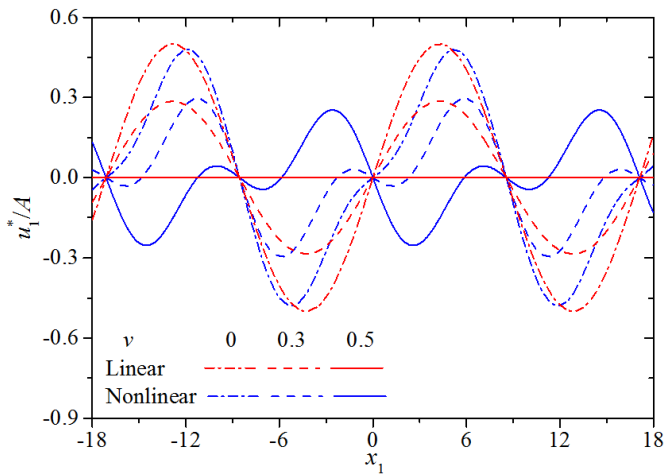


Figure 5: The tangential displacement of the substrate at the interface.

displacement of the substrate at the surface is shown in Fig. 5. When the substrate is incompressible ($\nu = 1/2$), u_1^* is zero in the linear model, but nonzero in the nonlinear model.

From Eq. (24), Fig. 6 shows the hyperelastic coefficient γ about the Poisson's ratio ν . It ranges from 0.029 ($\nu \approx 0.31$) to 0.047 ($\nu = 0.1$). From Eq. (23), the ratio of the strain energy of the substrate in two models is $\phi_s = 1 + \gamma A^2 k^2 = 1 + 4\gamma\pi^2 \delta^2 > 1$. The strain energy of the substrate in the nonlinear model is large than that in the linear model. With the increment of the Poisson's ratio ν , the energy ratio ϕ_s decreases first and then increases, as shown in Fig. 7(a). When $\nu \approx 0.31$, the energy ratio ϕ_s reaches the minimum. With the increment of δ , the energy ratio ϕ_s increases, as shown in Fig. 7(b).

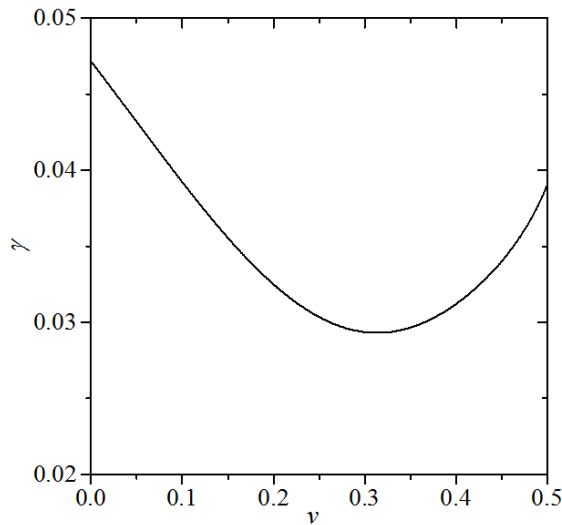


Figure 6: The hyperelastic coefficient γ .

4.2 Buckling

For the silicon film and PDMS substrate, the material and geometric parameters are $E_f = 130\text{GPa}$, $\nu_f = 0.28$, $E = 1.8\text{MPa}$, $\nu = 0.48$, $h = 0.1\mu\text{m}$, $l = 1\text{mm}$. The buckling features under different prestrains are obtained according to Eq. (35) and (29), as shown in Tab. 1

Fig. 8 shows the buckling wave number and amplitude about the prestrain ε in two models In the linear model, the buckling wave number k is constant But in the nonlinear model, the wave number increases with the increment of prestrain, as

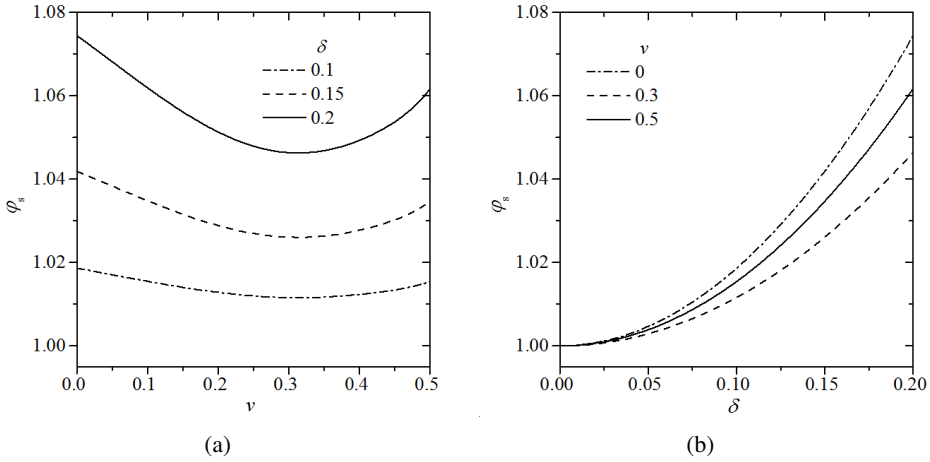


Figure 7: The ratio of substrate's strain energy between two models about (a) the Poisson's ratio and (b) $\delta = A/\lambda$.

Table 1: The buckling features in two models.

ε	$k(\mu\text{m}^{-1})$			$A(\mu\text{m})$		
	0.1	0.3	0.5	0.1	0.3	0.5
Nonlinear	0.407	0.487	0.571	1.628	2.563	3.032
Linear	0.367	0.367	0.367	1.717	2.977	3.844

shown in Fig. 8(a) The buckling amplitude A in the nonlinear model is less than that in the linear model, as shown in Fig. 8(b) With the increment of Poisson's ratio ν , the buckling wave number increase, but the amplitude decreases as shown in Fig. 9. The stronger the compressibility of the substrate (the less Poisson's ratio) is, the larger the amplitude and wavelength will be.

Fig. 10 shows the ratios of the buckling wave number κ , amplitude α and total energy ϕ between two models about the prestrain. With the increment of prestrain, the ratios of buckling wave number κ and total energy ϕ are larger than one and increase, but the ratio of amplitude α is less than one and decreases. The ratios of buckling wave number κ and amplitude α change significantly when the prestrain increase

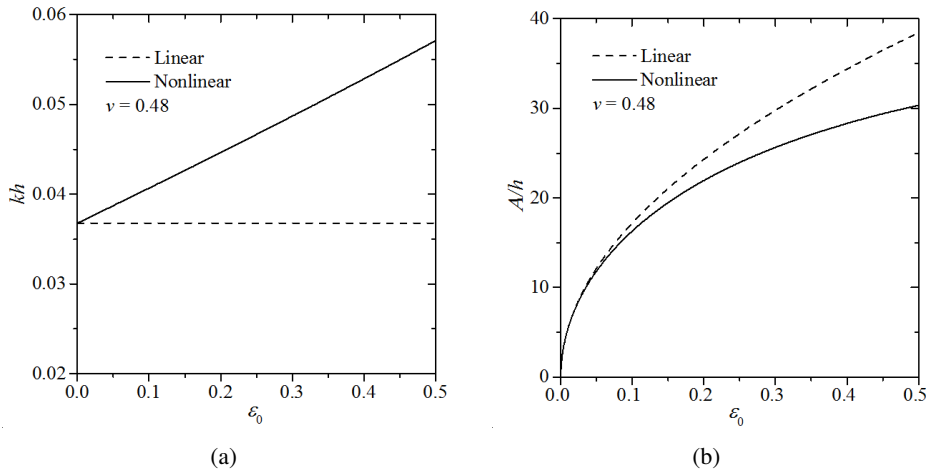


Figure 8: The buckling (a) wave number and (b) amplitude about the prestrain in two models.

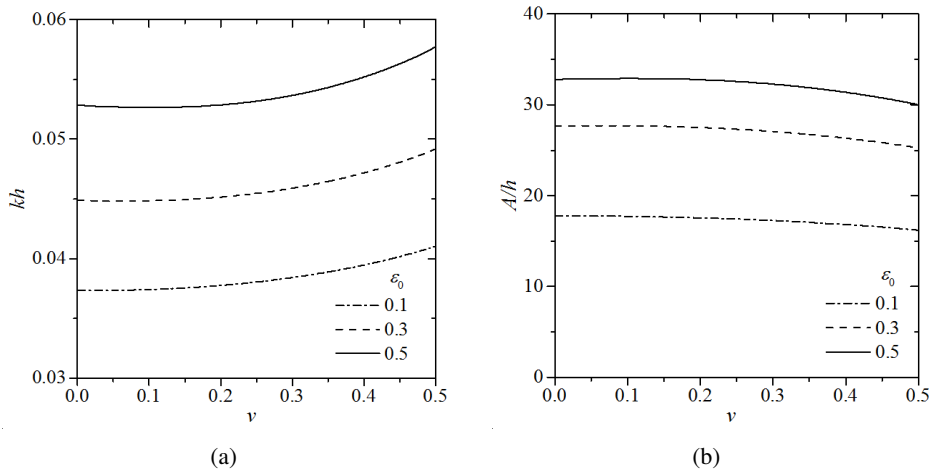


Figure 9: The buckling (a) wave number and (b) amplitude about Poisson's ratio in the nonlinear model.

4.3 Film

From Eq. (5), the midplane displacement of the film consists of two parts. Parts of the wavy displacements caused by buckling in two models are

$$\begin{aligned} \tilde{u}_1^f &= \frac{1}{8} \xi \tilde{A}^2 \tilde{k} \sin(2\tilde{k}x_1) \quad \text{in nonlinear model} \\ \tilde{u}_1^f &= \frac{1}{8} \tilde{A}^2 \tilde{k} \sin(2\tilde{k}x_1) \quad \text{in linear model} \end{aligned} \tag{36}$$

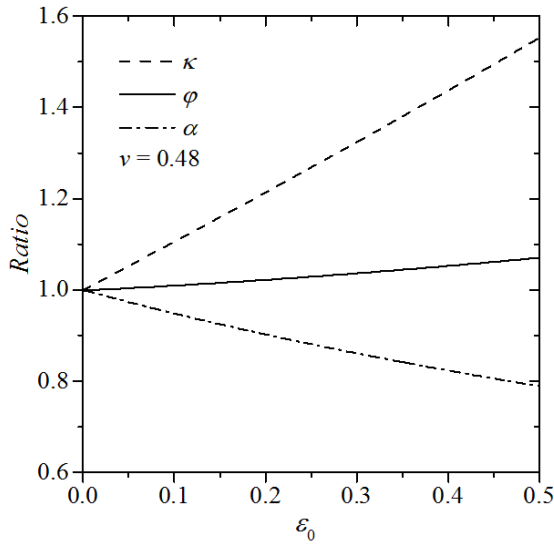


Figure 10: The ratio of wave number κ , amplitude α and total energy φ between two models about the prestrain.

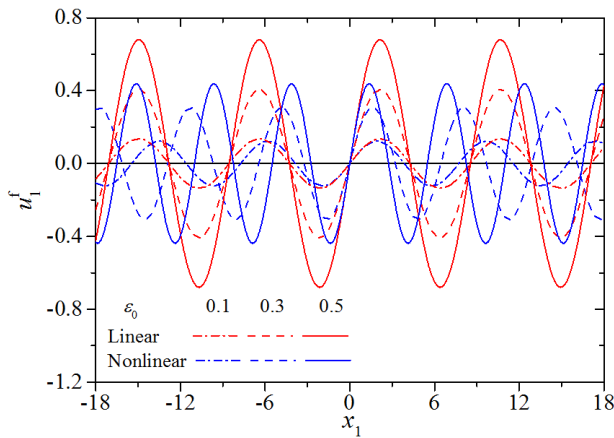


Figure 11: The wavy displacement of the film caused by buckling.

They are shown in Fig. 11 Comparing with the linear model, the prestrain not only influences the amplitude but also the wavelength. The larger the prestrain is, the shorter the wavelength will be in the nonlinear model. The amplitude in the nonlinear model is smaller than that in the linear model, and when the prestrain increase, such difference becomes remarkable.

5 Conclusion

This paper studies the buckling of the film and substrate structure in large deformation. A nonlinear model is developed. The film and the substrate are described by finite deformation theory under different original strain-free configurations. The neo-Hookean constitutive relation is applied to describe the substrate. Through the perturbation analysis, the displacement of the substrate under a uniaxial prestrain is obtained. The buckling wave number, amplitude and critical condition are obtained by energy method.

The displacement fields near the interface are different in two models. The strain energy of the substrate in the nonlinear model is large than that in the linear model. Comparing with the traditional linear model, the buckling amplitude in the nonlinear model decreases, but the wave number increases and relates to the prestrain. In the nonlinear model, the stronger the compressibility of the substrate is, the larger the buckling amplitude and wavelength will be.

Acknowledgement: This work was partially supported by the National Natural Science Foundation of China (Nos. 11372113 and 11472110) New Century Excellent Talents (No. NCET-13-0218).

References

- Audoly, B.; Boudaoud, A.** (2008): Buckling of a stiff film bound to a compliant substrate—Part I: Formulation, linear stability of cylindrical patterns, secondary bifurcations. *Journal of the Mechanics and Physics of Solids*, vol. 56, no. 7, pp. 2401-2421.
- Cai, S.; Breid, D.; Crosby, A. J.; Suo, Z.; Hutchinson, J. W.** (2011): Periodic patterns and energy states of buckled films on compliant substrates. *Journal of the Mechanics and Physics of Solids*, vol. 59, no. 5, pp. 1094-1114.
- Chen, X.; Hutchinson, J. W.** (2004): Herringbone buckling patterns of compressed thin films on compliant substrates. *Journal of Applied Mechanics-Transactions of the Asme*, vol. 71, no. 5, pp. 597-603.
- Huang, R.** (2005): Kinetic wrinkling of an elastic film on a viscoelastic substrate. *Journal of the Mechanics and Physics of Solids*, vol. 53, no. 1, pp. 63-89.
- Huang, R.; Suo, Z.** (2002): Instability of a compressed elastic film on a viscous layer. *International Journal of Solids and Structures*, vol. 39, no. 7, pp. 1791-1802.
- Huang, Z. Y.; Hong, W.; Suo, Z.** (2005): Nonlinear analyses of wrinkles in a film bonded to a compliant substrate. *Journal of the Mechanics and Physics of Solids*, vol. 53, no. 9, pp. 2101-2118.

- Im, S. H.; Huang, R.** (2008): Wrinkle patterns of anisotropic crystal films on viscoelastic substrates. *Journal of the Mechanics and Physics of Solids*, vol. 56, no. 12, pp. 3315-3330.
- Jiang, H. Q.; Khang, D. Y.; Fei, H. Y.; Kim, H.; Huang, Y. G.; Xiao, J. L.; Rogers, J. A.** (2008): Finite width effect of thin-films buckling on compliant substrate: Experimental and theoretical studies. *Journal of the Mechanics and Physics of Solids*, vol. 56, no. 8, pp. 2585-2598.
- Khang, D. Y.; Jiang, H. Q.; Huang, Y.; Rogers, J. A.** (2006): A stretchable form of single-crystal silicon for high-performance electronics on rubber substrates. *Science*, vol. 311, no. 5758, pp. 208-212.
- Kurapati, S.; Lu, Y.; Yang, F.** (2010): Indentation Load-Displacement Relations for the Spherical Indentation of Elastic Film/Substrate Structures. *Computers, Materials & Continua*, vol. 20, no. 1, pp. 1-17.
- Nair, A. K.; Farkas, D.; Kriz, R. D.** (2008): Molecular dynamics study of size effects and deformation of thin films due to nanoindentation. *Computer Modeling in Engineering & Sciences*, vol. 24, no. 2/3, pp. 239.
- Rogers, J. A.; Bao, Z.** (2002): Printed plastic electronics and paperlike displays. *Journal of Polymer Science Part A: Polymer Chemistry*, vol. 40, no. 20, pp. 3327-3334.
- Schubert, M. B.; Werner, J. H.** (2006): Flexible solar cells for clothing. *Materials Today*, vol. 9, no. 6, pp. 42-50.
- Song, J.; Jiang, H.; Choi, W. M.; Khang, D. Y.; Huang, Y.; Rogers, J. A.** (2008): An analytical study of two-dimensional buckling of thin films on compliant substrates. *Journal of Applied Physics*, vol. 103, no. 1, pp. 014303-014310.
- Song, J.; Jiang, H.; Liu, Z. J.; Khang, D. Y.; Huang, Y.; Rogers, J. A.; Lu, C.; Koh, C. G.** (2008): Buckling of a stiff thin film on a compliant substrate in large deformation. *International Journal of Solids and Structures*, vol. 45, no. 10, pp. 3107-3121.
- Wagner, S.; Lacour, S. P.; Jones, J.; Hsu, P.-h. I.; Sturm, J. C.; Li, T.; Suo, Z.** (2004): Electronic skin: architecture and components. *Physica E: Low-dimensional Systems and Nanostructures*, vol. 25, no. 2-3, pp. 326-334.
- Zhang, Q.; Yang, Q.-S.** (2013): The Analytical and Numerical Study on the Nanoindentation of Nonlinear Elastic Materials. *Computers, Materials & Continua*, vol. 37, no. 2, pp. 123-134.
- Zhu, L.; Zhou, J.; Fan, X.** (2014): Rupture and Instability of Soft Films due to Moisture Vaporization in Microelectronic Devices. *Computers, Materials & Continua*, vol. 39, no. 2, pp. 113-134.

